PERGAMON

Microelectronics Reliability 41 (2001) 605–610

MICROELECTRONICS RELIABILITY

www.elsevier.com/locate/microrel

Research note

Determination of trap cross-section in a-Si:H p-i-n diodes parameters using simulation and parameter extraction

Magali Estrada [a,*], Antonio Cerdeira [a], Adelmo Ortiz-Conde [b,1], Francisco García [b]

[a] *Sección de Electrónica del Estado Sólido, Departamento de Ingeniería Eléctrica, CINVESTAV-IPNAv. IPN No. 2508, Apto 14-740, 07300 México, Mexico*

[b] *Laboratorio de Electrónica del Estado Sólido, Universidad Simón Bolivar, Apartado Postal 8900, Caracas 1080A, Venezuela*

Received 23 November 2000; received in revised form 22 December 2000

Abstract

Modeling the current density–voltage (J–V) curve of a-Si:H p-i-n diodes requires a group of input physical parameters that have to be previously determined. Some of them can be determined directly from experiment, while others, as the trap cross-section, have to be indirectly determined or assigned. We present a simple procedure to estimate trap cross-section using computer simulation and parameter extraction. The experimental J–V forward characteristic of the p-i-n diode, dark and illuminated, is used to determine the ideality factor n and the short circuit current density J_{SC}. The charged trap cross-section and its relation to the neutral trap cross-section are determined by fitting to tabulated and graphical results from simulation. Determined values of trap cross-section are used to simulate the reverse current of diodes under illumination and results compared with experimental curves. © 2001 Elsevier Science Ltd. All rights reserved.

1. Introduction

a-Si:H p-i-n diodes have been investigated as radiation detectors, where incident radiation can go from visible light to high energy radiation. The p-i-n diode is usually made by depositing an n^+-layer, followed by an intrinsic and a p^+-layer. The doped n^+- and p^+-layers are usually less than 400 nm, but the intrinsic (i-layer) can go from tenth to tens of micrometers, in dependence of the application.

Photodiodes and image sensors have up to several micrometers of i-layer, while particle and nuclear radiation detectors need much thicker i-layers, of tens or hundreds of micrometers. The reverse dark current at the operating voltage defines the threshold of detection. This dark current as well as the selection of the operating voltage will depend on a high extent on the electric field distribution inside the structure, which is tightly related to the density and energy distribution of localized states inside the mobility gap, as well as other physical parameters of the a-Si:H structure. The reverse diode current also depends on the trap cross-section.

Analytical and numerical modeling of the current density–voltage (J–V) characteristic of a-Si:H p-i-n have been presented in many works (see e.g. Refs. [1–3]), specially related to solar cells. Simulation provides a mean to study and understand the behavior of the device and the factors that limit its efficiency, if the model used to describe the device behavior is sufficiently precise and physical input parameters required by the simulator are known. Mobility (μ_n and μ_p); charged and neutral cross-sections of deep and tail states (σ_{Cd}, σ_{Nd}, σ_{Ct}, σ_{Nt}); activation energy of states; band gap E_g and constant density of charged states at full depletion N_0 must be known. Technological and geometrical parameters are also required. Some of these parameters can be determined by different electrical and optical measurements,

* Corresponding author.
E-mail address: mestrada@mail.cinvestav.mx (M. Estrada).

[1] On sabbatical leave from Universidad Simón Bolivar.

0026-2714/01/$ - see front matter
PII: S0026-2714(01)00005-1

while others, as the trap cross-sections have to be indirectly determined or assumed. The characteristics of a-Si:H devices are deeply related to trapping and recombination mechanisms, due to the presence of a relatively high density of localized traps inside the mobility gap of the material, so the model used in simulation must include a correct characterization of these traps. Since the trap cross-section is highly dependent on fabrication technology, it must be determined for the technological process in use. Indirect methods of trap cross-section determination can introduce inaccuracies because different structures from the one to be evaluated have to be specially prepared for them. Method proposed in this work has the advantage of allowing the determination of the trap cross-section in the same devices that are to be characterize as photodetectors. Simulation, once validated, can be also used to see how variations on the technological process affect the trap characteristics and device behavior.

In this work we present a procedure to determine the neutral and charged cross-section of deep states using parameter extraction from the experimental *J–V* curves in conjunction with results from simulation. An example is presented to demonstrate that estimated parameters fit well with expected.

2. Simulation of a-Si:H p-i-n devices

The forward and reverse current, both dark an under illumination, of amorphous p-i-n diodes with intrinsic layer thickness W from 0.7 to 17.5 μm were simulated in ATLAS [4]. In a previous work [5] we showed problems found when simulating these devices using ATLAS. The gaussian distribution of states (DOS) distribution used in the default model locates the Fermi level at the middle of the gap, instead of the normally reported location around 0.2 eV above it. For this reason the electric field distribution inside amorphous a-Si:H devices resulted very similar to that of a crystalline diode with a substrate concentration of impurities equal to the constant density of charged states at the a-Si:H layer at full depletion and a band gap corresponding to the a-Si:H material. All other electrical characteristics simulated will differ from reality since they are based on the electric field distribution. To take into account features inherent to amorphous materials, the default model has to be disabled and the expected DOS in the amorphous material must be introduced in the program using Silvaco's tool "C-Interpreter". The activation energy, cross-section and density of acceptor tails, donor tails, acceptor deep and donor deep states must be independently described for each species. These parameters are quite sensitive to device fabrication.

Among different descriptions of trap distribution we selected the exponential dependence of tails and deep states reported in Ref. [6]. The energy distribution of acceptor and donor tail states is given by Eqs. (1) and (2) respectively, while the distribution of deep acceptor and donor states is given by Eqs. (3) and (4).

$$g_{at} = g_{ato} \ \exp(-(E_C - E)/E_{at}), \tag{1}$$

$$g_{dt} = g_{dto} \ \exp(-(E_V - E)/E_{dt}), \tag{2}$$

$$g_{ad} = g_{ado} \ \exp(-(E_C - E)/E_{ad}), \tag{3}$$

$$g_{dd} = g_{ddo} \ \exp(-(E_V - E)/E_{dd}), \tag{4}$$

where E_C and E_V are the conduction and valence band energy.

The density of acceptor and donor tail and deep states were taken as in Ref. [3]: $g_{ato} = g_{dto} = 2 \times 10^{20}$ cm^{-3}; $g_{ado} = 4 \times 10^{18}$ cm^{-3} and $g_{ado} = 6 \times 10^{18}$ cm^{-3}. The activation energy for acceptor and donor tail and deep states was also taken as [3]: $E_{at} = 0.034$ eV; $E_{dt} =$ 0.054 eV; $E_{dd} = 0.1289$ eV and $E_{ad} = 0.0879$ eV to fit experiment. Other features of the model used in this simulator can be found in Ref. [4].

To analyze how some of the above mentioned parameters (activation energy, cross-section and density of each trap species) affected the *J–V* characteristic of the device, we made simulations varying their values in ranges usually reported in literature. Values of charged σ_{Cd} and neutral cross-section σ_{Nd} of deep states were varied from 10^{-13} to 10^{-16} cm^{-2}; the ratio of $\xi = \sigma_{Cd}/\sigma_{Nd}$ was varied from 10 to 1000. Simulation was also made for values of hole mobility μ_p varying from 0.005 up to 0.5 cm^2/V s. The ratio of electron to hole mobility was varied from 10 to 1000. The intensity of light was varied from 0.001 up to 30 mW/cm^2. The impurity concentration in both p^+- and n^+-regions was considered of 10^{18} cm^{-3} from experimental data. The energy gap of 1.72 eV and the Fermi level located 0.2 eV above the middle of the gap, were obtained from experimental data for devices fabricated in our laboratory. The constant density of charged states in the amorphous diode at deep depletion, N_0, was estimated to be 10^{15} cm^{-3} using previously reported methods [7].

In Ref. [8] it was shown that the reverse dark current of a-Si:H p-i-n diodes starts to increase more rapidly with voltage above a critical electric field of 4×10^4 V/cm, due to field enhanced factors affecting it. Atlas does not take into account these effects so the *J–V* curve obtained from ATLAS must be post-processed using the expressions presented in Ref. [8]. The typical exponential dependence of the Pool–Frenkel effect was described as:

$$f(V) = e^{\beta\sqrt{F(V)}} + e^{\gamma F(V)}, \tag{5}$$

where $\beta = 0.008835$ $(cm/V)^{0.5}$ is the Pool–Frenkel constant normalized to kT and where $\gamma = qs/kT$ (V/cm) is the factor due to multiple emission from centers located at a distance s.

3. Results from simulation

Once the trap distribution is selected, from simulation results for different input data, the influence of the trap cross-section on the J–V characteristic can be obtained. The ideality factor n, the saturation current J_0, the open collector voltage V_{OC} and the short circuit current density J_{SC} were calculated for different set of input parameters.

3.1. Forward J–V curve without illumination

Results from simulation indicate that the ideality factor n depends mainly on σ_{Cd} and ζ. A small dependence with μ_p is also observed for $\mu_p < 0.01$ cm^2/V s and there is practically no dependence with μ_n. Cross-section of charged and neutral tail states have very little influence on both n and J_0.

Fig. 1 shows the dependence of n with σ_{Cd} and ζ; that allows us to interpolate and estimate the values that best fit experiment. This result from simulation could be expected from the physical processes that affect n.

3.2. The J–V curve under illumination

This curve has two important parameters for our purpose, the open collector voltage V_{OC} and the short circuit current density J_{SC}. Both of them depend on the light power density P_W in mW/cm^2, σ_{Cd} in cm^2 and ζ as indicated in Figs. 2 and 3.

Analyzing the behavior of V_{OC} as function of trap cross-section and light power density P_W and fitting the proposed dependence to the simulated curves, the following analytical relationship was found:

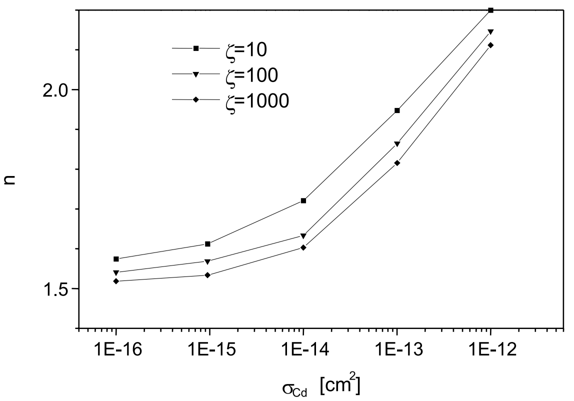

Fig. 1. Dependence of n with σ_{Cd} for different values of ζ.

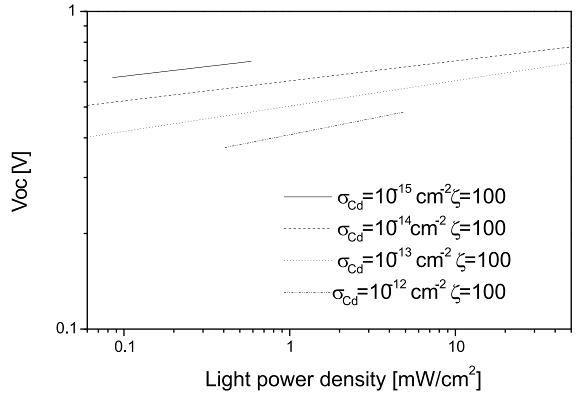

Fig. 2. Dependence of V_{OC} with light power density for different pairs of values of σ_{Cd} and ζ.

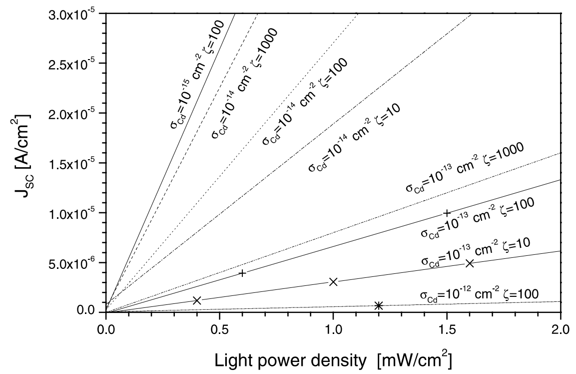

Fig. 3. Dependence of J_{SC} with light power density for different pairs of values of σ_{Cd} and ζ.

$$V_{OC} = V_0 \log\left(1 + \frac{P_W}{C_1\ \sigma_{Cd}}\right), \tag{6}$$

where $V_0 = 0.093$ V and $C_1 = 2 \times 10^7$ mW/cm^4 for and $\xi = 100$, $\mu_p = 0.001$ cm^2/V s and $\mu_n/\mu_p = 100$.

Fig. 3 shows that J_{SC} depends linearly with P_W, where the value of the slope for different pairs of σ_{Cd} and ζ is indicated in Table 1. Table 2 shows the values of $d J_{SC}/d\sigma_{Cd}$ for different light power densities, An analytical expression was also found to relate J_{SC} with σ_{Cd} and ζ to simplify the adjustment procedure. For example for $\xi = 100$, $\mu_p = 0.001$ cm^2/V s and $\mu_n/\mu_p = 100$:

$$J_{SC} = C_2\ P_W\left[1 + 7\ \log\left(\frac{\sigma_0}{\sigma_{Cd}}\right) + 11.4\ \log^2\left(\frac{\sigma_0}{\sigma_{Cd}}\right)\right], \tag{7}$$

where $C_2 = 4.3 \times 10^7$ A/mW and $\sigma_0 = 10^{-12}$ cm^2

Simulation also indicates that increasing μ_p again slightly increases J_{SC}, but variations on μ_n, practically have no influence.

Table 1
dJ_{SC}/dP_W for different values of σ_{Cd} and ζ

σ_{Cd}	ζ	dJ_{SC}/dP_W
10^{-12}	100	5.2×10^{-7}
10^{-13}	10	3.1×10^{-6}
–	100	5.9×10^{-6}
–	1000	8×10^{-6}
10^{-14}	10	1.8×10^{-5}
–	100	2.7×10^{-5}
–	1000	2.9×10^{-5}
10^{-15}	100	5.2×10^{-5}

Table 2
$dJ_{SC}/d\sigma_{Cd}$ for different values of light intensity and μ_n and μ_p

P_W (mW/cm^2)	$dJ_{SC}/d\sigma_{Cd}$	μ_p	μ_n
0.1	-2.38×10^{-6}	0.01	1
0.2	-4.6×10^{-6}	0.01	1
0.3	-6.8×10^{-6}	0.01	1
0.4	-8.98×10^{-6}	0.01	1
0.5	-1.14×10^{-6}	0.01	1
0.5	-1.5×10^{-6}	0.05	1
0.5	-1.14×10^{-6}	0.01	0.5

4. Procedure for estimating basic parameters

First step in determining trap cross-section consists in calculating the ideality factor n from the experimental dark J–V curve. Fig. 1 is then used to determine pairs of values of σ_{Cd} and ζ that can correspond to the calculated value of n.

It should be noticed that, since the amorphous device can have a very low current density for $V < 0.4$ V, the measurement installation or the leakage though the borders of the device structure, can give rise to a shunt resistance. The effect of the shunt resistance must be eliminated in order to calculate correctly the value of n. Poor ohmic contacts can also give rise to an undesirable non-linear series resistance. These effects alter the form of the measured forward J–V curve as can be seen in Fig. 4. There are several methods to calculate the correct parameters even in the presence of these non-desired effects [9–11]. Since in the presence of a series non-linear resistance the value of the saturation current J_0 is altered due to the parallel displacement along the y-axis of the J–V curve, we will only use the determination of the ideality factor n in our procedure.

Afterwards, the short circuit current J_{SC} is determined from the experimental illuminated J–V curve, where P_W is known. Using Fig. 3 as well as Tables 1, 2 and Eq. (7), for same values of σ_{Cd} and ζ, J_{SC} is determined from simulation results for the measured light intensity P_W (Fig. 2 and Eq. (7)). Finally, the pair of values of σ_{Cd} and that best fit experiment is selected. Further adjustment can be made varying μ_p.

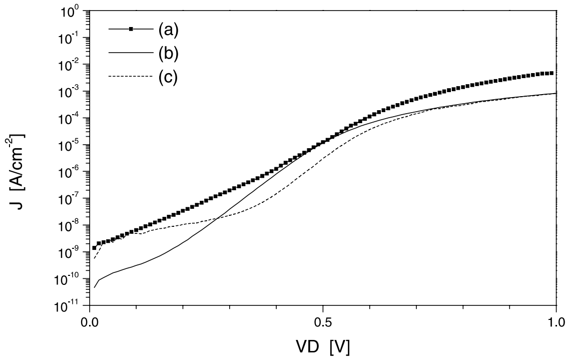

Fig. 4. Forward J vs V_D diode characteristic showing: (a) the effect of the diode series resistance; (b) the effect of a shunt resistance in parallel to the diode; (c) same as (a) plus the effect of non-ohmic contact.

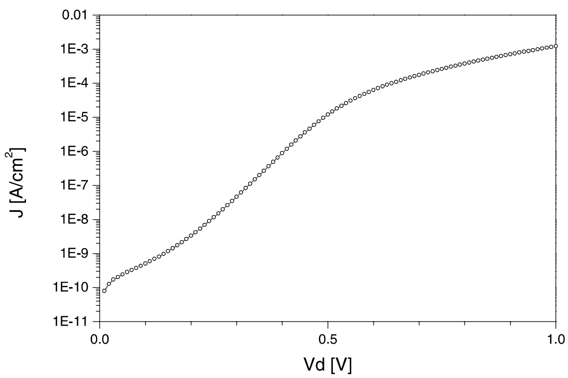

Fig. 5. Forward current vs voltage of an a-Si:H diode showing the effect of a shunt resistance.

The procedure for estimating the trap capture cross-sections is shown in the example of an a-Si:H diode 0.7 μm thick. The forward J–V current of an a-Si:H diode is shown in Fig. 5. At the origin, a small effect of shunt resistance and non-ohmic contact already indicated is seen. Using the procedure indicated in Ref. [9], a value of the ideality factor of the a-Si:H diode $n = 1.6$ was determined.

The procedure in Ref. [9] consists in solving the value of the current I for a circuit consisting of a shunt resistance in parallel to two diodes including their series resistance, one representing the non-ohmic contact and the other the a-Si:H diode. For low voltages, usually the non-ohmic contact is limiting the current in this branch and its basic parameters (n_1 and J_{01}) can be determined directly or using the procedure indicated in Ref. [10] if a shunt resistance is present. For higher voltages, it is demonstrated that the current through the two diodes can be expressed as:

$$I \approx I_{01}^{n_1/(n_1+n_2)} \, I_{02}^{n_2/(n_1+n_2)} \, \exp\left[\frac{V}{(n_1+n_2)} \frac{q}{kT}\right]. \quad (8)$$

So the value of n_2, corresponding in our case to the ideality factor of the a-Si:H diode, can be determined from the measured *I–V* curve.

From Fig. 1, three pairs of values of σ_{Cd} and ζ can be chosen for the measured n: $\sigma_{Cd} = 8 \times 10^{-16}$ cm^2, $\xi = 10$; $\sigma_{Cd} = 8 \times 10^{-15}$ cm^2, $\xi = 100$ and $\sigma_{Cd} = 1.6 \times 10^{-14}$ cm^2, $\xi = 1000$.

Experimentally J_{SC} was determined to be 8.9×10^{-6} and 2.22×10^{-4} A/cm^2 for two light intensity. The device was illuminated with a filtered, collimated, 68 nm wavelength light though a optical fiber. The smaller light intensity generating e–h pairs at the i-layer was of approximately 0.3 mW/cm^2 and the higher of approximately 10 mW/cm^2. The incident light intensity illuminating the device was measured using a semiconductor "Smartsensor" coupled to a "FieldMaster" meter; the intensity absorbed at the i-layer was estimated after considering losses in the Cr, and p-region as well as back metal reflection. For typical values of $\mu_n = 1$ cm^2/V s and $\mu_p = 0.01$ cm^2/V s the measured and simulated reverse *J–V* characteristics are compared. Determined values of σ_{Ct} and ζ were used to simulate the reverse current of the illuminated photodiode. Fig. 6 shows the comparison between experimental and simulated reverse current curves for the diode. For the low power curve, the correspondence is excellent, indicating that the estimated values of the trap cross-section represent quite well the trap characteristics of the device. For higher light intensity, there is a small deviation indicating that some other factor is also affecting.

The procedure indicated above, can be used for any a-Si:H p-i-n diode, with an i-layer thickness W for which the mean electric field across the i-layer $F_{mean} > 3 \times 10^3$ V/cm in the absence of external bias. As indicated in Fig. 7 for smaller F_{mean}, the J_{SC} will decrease as the field is decrease, or what is the same, will decrease with increasing W. This can be understood from the discussion of the electric field distribution inside these diodes, presented in Ref. [8].

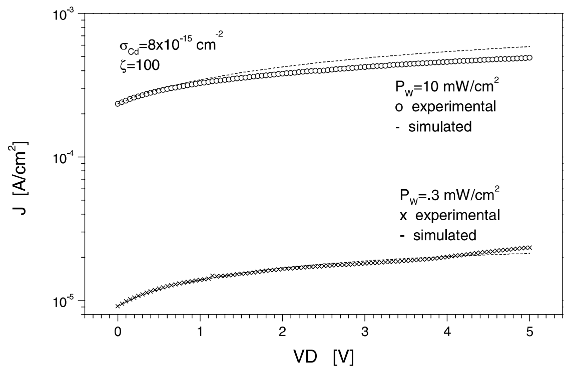

Fig. 6. Comparison of experimental and simulated reverse current under illumination for an a-Si:H diode after determination of the trap cross-section by the present method.

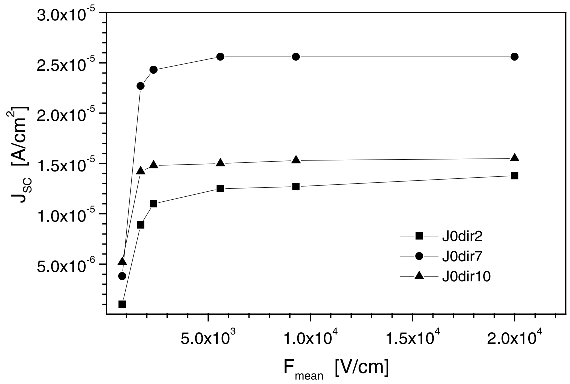

Fig. 7. Dependence of the short circuit current on the mean electric field present across the i-layer of the p-i-n diode.

Determination of σ_{Ct} and σ_{Nt} has been previously done using V_{OC} [12]. However authors use it to determine the cross-section of tail states. Our results indicate, on the contrary, that tails states have very little influence on V_{OC}, compared to deep states, as should be expected also from physical interpretation of their influence. In addition the simulated and experimental values of V_{OC} also differ even when the illuminated reverse current is quite satisfactorily simulated indicating the presence of other effects mentioned by same authors.

5. Conclusions

A procedure to estimate trap capture cross-section in a-Si:H is presented. The experimental *J–V* forward characteristic is used to determined the ideality factor n and the short circuit current J_{SC}. Charged and neutral trap capture cross-sections are obtained from tabulated and graphical results from simulation, looking for best values that fit the experimentally determined values of n and J_{SC}.

Simulated reverse current under illumination using the trap cross-section determined by this method shows very good correspondence with experiment, indicating that validity of the procedure.

Since these parameters are quite important for the correct description of the a-Si:H devices the above described procedure has the advantages that, once tabulated and graphical results from simulation are available, the procedure is simple and precise without loosing the physical understanding of the behavior of the devices.

Acknowledgements

This work was supported by CONACYT projects 34400-A and 28092A and CONICIT grant N1 S1-9800567. We thank Olga Gallegos at SEES CINVESTAV for sample preparation and Hector Baez and Brenda Garcia for diode characterization.

References

[1] Mittiga A, Fiorini P, Falconieri M, Evangelisti F. Dark *J–V* characteristic of PIN a-Si:H solar cells. J Appl Phys 1989;66(6):2667.
[2] Hack M, Shur M. Theoretical modeling of amorphous silicon-based alloy p-i-n solar cells. J Appl Phys 1983;54(10):5858.
[3] Su CY, Hwang HL. Simulation and analysis of amorphous silicon image sensor having a p-i-n structure. Solid-State Electron 1992;35(12):1811.
[4] ATLAS User's Manual, Silvaco International, February 2000.
[5] Cerdeira A, Estrada M, Baez H, Aleman M. Analytical and numerical modeling of the electric field distribution in amorphous thin and thick p-i-n diodes. Third Workshop on Simulation and Characterization Techniques, Mexico D.F., 6–7 September, 1999. p. 27–30.
[6] Tsai Y, Hong K, Yuan Y. An efficient analytical model for calculating trapped charge in amorphous silicon. IEEE Trans Comput-Aided Des Integrat Circ Syst 1994; 13(6):725.
[7] Street RA. Physics of a-Si:H pin devices. J Non-Cryst Sol 1993;164-166:643.
[8] Cerdeira A, Estrada M. Modeling of reverse current behavior in amorphous thin and thick p-i-n diodes. Trans Electron Dev 2000;41(11):2338.
[9] Ortiz-Conde A, Estrada M, Cerdeira A, García F, DeMercato G. A series combination of two ideal diodes with parallel resistance for modeling real devices and its parameter extraction, in press.
[10] Ranuarez JC, Ortiz-Conde A, García FJ. A new method to extract diode parameters under the presence of parasitic series and shunt resistance. Microelectron Reliab 2000;40:355.
[11] García F, Sanchez A, Ortiz-Conde JJ. A parasitic series resistance-independent method for device-model parameter extraction. IEEE Proc Circ Dev Syst 1996; 143:68.
[12] Sakata I, Hayashi Y. Theoretical analysis of trapping and recombination of photogenerated carriers in amorphous silicon solar cells. J Appl Phys A 1985;37:153.